Atmos. Chem. Phys., 10, 463–474, 2010
www.atmos-chem-phys.net/10/463/2010/

Atmospheric Chemistry and Physics

Kinetics and mechanisms of heterogeneous reaction of NO_2 on $CaCO_3$ surfaces under dry and wet conditions

H. J. Li, T. Zhu, D. F. Zhao, Z. F. Zhang, and Z. M. Chen

State Key Joint Laboratory of Environmental Simulation and Pollution Control, College of Environmental Sciences and Engineering, Peking University, Beijing, 100871, China

Received: 7 January 2009 – Published in Atmos. Chem. Phys. Discuss.: 17 March 2009
Revised: 15 December 2009 – Accepted: 16 December 2009 – Published: 20 January 2010

Abstract. With increasing NO_2 concentration in the troposphere, the importance of NO_2 reaction with mineral dust in the atmosphere needs to be evaluated. Until now, little is known about the reaction of NO_2 with $CaCO_3$. In this study, the heterogeneous reaction of NO_2 on the surface of $CaCO_3$ particles was investigated at 296 K and NO_2 concentrations between 4.58×10^{15} molecules cm^{-3} to 1.68×10^{16} molecules cm^{-3}, using diffuse reflectance infrared Fourier transform spectroscopy (DRIFTS) combined with X-ray photoelectron spectroscopy (XPS) and scanning electron microscopy (SEM), under wet and dry conditions. Nitrate formation was observed under both conditions, while nitrite was observed under wet conditions, indicating the reaction of NO_2 on the $CaCO_3$ surface produced nitrate and probably nitrous acid (HONO). Relative humidity (RH) influences both the initial uptake coefficient and the reaction mechanism. At low RH, surface −OH is formed through dissociation of the surface adsorbed water via oxygen vacancy, thus determining the reaction order. As RH increases, water starts to condense on the surface and the gas-liquid reaction of NO_2 with the condensed water begins. With high enough RH (>52% in our experiment), the gas-liquid reaction of NO_2 with condensed water becomes dominant, forming HNO_3 and HONO. The initial uptake coefficient γ_0 was determined to be $(4.25\pm1.18)\times10^{-9}$ under dry conditions and up to $(6.56\pm0.34)\times10^{-8}$ under wet conditions. These results suggest that the reaction of NO_2 on $CaCO_3$ particle is unable to compete with that of HNO_3 in the atmosphere. Further studies at lower NO_2 concentrations and with a more accurate assessment of the surface area for calculating the uptake coefficient of the reaction of NO_2 on $CaCO_3$ particle and to examine its importance as a source of HONO in the atmosphere are needed.

Correspondence to: T. Zhu
(tzhu@pku.edu.cn)

1 Introduction

It has been estimated that 1000–3000 Tg of mineral aerosols are emitted into the atmosphere annually (Jonas et al., 1995). The main components of mineral dust include quartz, feldspar, carbonate (e.g. calcite, dolomite) and clay. Each of these components provides surfaces and reactants for heterogeneous reactions in the atmosphere. Many gas phase species in the atmosphere could also condense or adsorb onto mineral dust during long-range transport to impact atmospheric chemistry and climate change (Chen, 1985; Quan, 1993; Carmichael et al., 1996; Zhang et al., 2000). Modeling studies suggested that approximately 40% of nitrate formation is associated with mineral aerosols (Dentener et al., 1996). Aerosol samples taken in East Asia showed a good correlation between nitrate and calcium (Zhuang et al., 1999; Song and Carmichael, 2001; Sullivan et al., 2007).

In fresh Asian mineral aerosols, calcium is found primarily in the form of calcium carbonate ($CaCO_3$) (Song et al., 2005; Okada et al., 2005). The observed association of nitrate with calcium in mineral dust samples after long range transport suggests that after exposure to nitrogen oxides in polluted region, calcium carbonate in mineral dust had been converted

Published by Copernicus Publications on behalf of the European Geosciences Union.

to calcium nitrate, which in turn can change the composition and morphology of calcium-containing aerosols and enhance their hygroscopicity and the rates of heterogeneous reactions, thus influence atmospheric chemistry. Calcium nitrate can also alter the optical properties of aerosols to impact radiation, cloud formation, and global climate change.

Laboratory studies have demonstrated that nitric acid (HNO_3) can react with $CaCO_3$ to form calcium nitrate (Fenter et al., 1995; Goodman et al., 2000; Hanisch and Crowley, 2001; Krueger et al., 2003a, b). The measured uptake coefficient accounting for the BET area of the samples was determined to be $(2.5\pm1)\times10^{-4}$ for HNO_3 on $CaCO_3$ under dry conditions (Goodman et al., 2000). Johnson et al. (2005) determined the initial uptake coefficient of HNO_3 on $CaCO_3$ to be $(2\pm0.4)\times10^{-3}$. The net reaction probability of HNO_3 on $CaCO_3$ particles was found to increase with increasing relative humidity, from 0.003 at RH=10% to 0.21 at 80% (Liu et al., 2008a). Vlasenko et al. (2006) reported an uptake coefficient of HNO_3 on $CaCO_3$ to be 0.11 at 33% relative humidity and a humidity dependence on Arizona Test Dust.

Compared to nitric acid, little is known about the reaction of NO_2 on $CaCO_3$. The uptake coefficients of NO_2 on mineral oxide particles, such as Al_2O_3, Fe_2O_3, TiO_2, have been determined to be on the order of 10^{-7} (Underwood et al., 1999), which is consistent with the results of the reaction of NO_2 on mineral dust samples from the Cape Verde Islands (Ullerstam et al., 2003). Boerensen et al. (2000) reported the reactive uptake coefficient of NO_2 on Al_2O_3 at levels of 10^{-9}.

No literature report about the uptake coefficient of NO_2 on $CaCO_3$ has been found. Considering that the concentration of NO_2 in the atmosphere is at least an order of magnitude higher than that of HNO_3, the reaction of $CaCO_3$ particles with NO_2 may comprise an important atmospheric reaction that lead to the formation of calcium nitrate during the long range transport of mineral dust. This reaction could be even more important in East Asia, where industrial regions with high NO_2 emissions are located in the path of long range transport of Asian Dust.

To understand the importance of the heterogeneous reaction of NO_2 on mineral dust, it is important to measure the uptake coefficient of NO_2 on $CaCO_3$ particles. Similar to the reaction of HNO_3 on $CaCO_3$, the reaction of NO_2 on $CaCO_3$ may also change under the influence of surface water. Therefore, it is interesting to study the reaction mechanisms and to measure the uptake coefficient of the reaction of NO_2 on $CaCO_3$ particles under dry and wet conditions.

In this study, the reactions of NO_2 on $CaCO_3$ surfaces was investigated in situ using diffuse reflectance infrared Fourier transform spectroscopy (DRIFTS) in combination with X-ray photoelectron spectroscopy (XPS), ion chromatography (IC), and scanning electron microscopy (SEM). Initial uptake coefficients were measured and the reaction mechanisms were studied under different relative humidity (RH).

2 Experimental

The infrared (IR) spectrum of the particle surface was investigated on line with DRIFTS during the reaction. The reactor of DRIFTS is a vacuum reaction chamber (Model HVC-DR2) surrounding a Harrick Scientific diffuse reflectance accessory (Model DRA-2CS) located in the sampling compartment of a Nicolet Nexus FTIR Spectrometer equipped with a mercury cadmium telluride (MCT) detector. Data from 128 scans, 4 cm^{-1} resolution, taken over about 80 s were averaged for one spectrum.

Besides online infrared spectroscopy measurements, for a number of selected experiments, the reaction products on the particle surface and extractable soluble components were also measured off line using X-ray photoelectron spectroscopy (XPS) and Ion Chromatography (IC), respectively. The morphological changes were observed using SEM. Further details of the instruments have been described previously (Li et al., 2006).

$CaCO_3$ (>99.999%, Alfa Aesar) powder was prepared by grinding and the size of the ground particle was about 1-10 µm with a mean value of 5.6 µm, as measured with a laser particle sizer (MasterSizer 2000, Malvern). The size and morphology of the ground $CaCO_3$ particles was also measured with SEM (KYKY1000B, KYKY Technology Development LTD., Beijing, China) (Fig. S1: http://www.atmos-chem-phys.net/10/463/2010/acp-10-463-2010-supplement.pdf). The ground $CaCO_3$ particles have various shapes; to simplify the estimation of surface area, we assumed the $CaCO_3$ particles have cubic shape. Using the size distribution measured with the laser particle sizer and using cubic shape for all $CaCO_3$ particles, the specific geometric surface area of the $CaCO_3$ particles (Ap) was calculated to be 0.19 $m^2\,g^{-1}$. The volumetric BET (Brunauer, Emmett and Teller model) surface area of particles was measured with an ASAP2010 BET apparatus (Micromeritics Co., USA). The BET surface area, A_{BET}, was determined to be 4.91 $m^2\,g^{-1}$, which is 25.8 times the specific geometric surface area Ap of $CaCO_3$ particles.

For experiments with DRIFTS, about 20 mg $CaCO_3$ particles was placed in the sample holder, pressed flat using a glass slide, and stored in a desiccator as previously described (Li et al., 2006). Water vapor was produced and gases were mixed using the apparatus displayed in Fig. S2: http://www.atmos-chem-phys.net/10/463/2010/acp-10-463-2010-supplement.pdf. All tubes and surfaces were made of inert glass or Teflon with the exception of the stainless steel in situ reactor. Concentrations of NO_2 entering the reactor were adjusted by mixing a NO_2 standard gas (710 ppm in N_2, Center of National Standard Material Research) with pure N_2 (>99.999%) using two mass flow controllers (FC-260, Tylan, Germany). The flow lifetime in the DRIFTS cell is 2 s. In the reactor, the NO_2 diffused to the particle surface and reacted with $CaCO_3$. The formation of the reaction products was monitored using DRIFTS. When we use SiO_2 particles to react with NO_2 as a control experiment under dry conditions, we did not detect NO_3^- formation.

Humidity was regulated by mixing dry nitrogen with water vapor by bubbling through two glass grits in pure water (Millipore Corporation, Billerica, MA, USA). Humidity was monitored using a temperature sensor (PT100; Vaisala, Vantaa, Finland) and a humidity sensor (HM1500; Vaisala).

After the reactions, the absolute numbers of nitrate and nitrite ions formed during the reaction were determined with IC. The reacted $CaCO_3$ particles were sonicated in 10 mL of pure water (Millipore Corporation), and then the filtered solution was analyzed using an IC (Dionex DX-500 system), which was equipped with an Ionpac AS-11HC-4 mm analytical column and a conductivity detector. Details of analyzing conditions can be found in a previous paper (Li et al., 2006).

The XPS spectra were taken on an AXIS-Ultra instrument from Kratos Analytical using monochromator Al K α radiation (225 W, 15 mA, 15 kV) and low-energy electron flooding for charge compensation. To compensate for surface charges effects, binding energies were calibrated using C1s hydrocarbon peak at 284.80 eV. The data were converted into VAMAS file format and imported into CasaXPS software package for data processing and curve-fitting.

3 Results

3.1 Reaction under dry conditions

Experiments under dry conditions were carried out by first heating the $CaCO_3$ at 623 K for 2 h, thus eliminating nearly all of the adsorbed water. A mixture of NO_2 and N_2 with no water vapor was admitted at 296 K.

Figure 1 shows typical IR spectra of $CaCO_3$ when reacted with NO_2 under dry conditions for 0 to 100 min. Nitrate was clearly observed on the $CaCO_3$ surface. The peak at 816 cm^{-1} was assigned to the out-of-plane bending of nitrate ν_2. The peak at 1043 cm^{-1} was assigned to the symmetric stretching of nitrate ν_1 and the peak at 748 cm^{-1} was assigned to the in-plane bending of nitrate ν_4. Peaks at 1295, 1330, and 1350 cm^{-1} were assigned to the asymmetric stretching of nitrate ν_3. The ν_3 mode of nitrate on the $CaCO_3$ surface has many peaks, which is different from that of the nitrate ions in $Ca(NO_3)_2$. This can be attributable to the degenerate ν_3 mode of adsorbed nitrate of different coordination with surface (monodentate, bidentate, and bridging) (Underwood et al., 1999).

The asymmetric stretching of adsorbed nitric acid has been reported to be at 1710/1680 cm^{-1} (Nakamoto, 1997; Finlayson-Pitts et al., 2003). In our study, to confirm the vibration frequency of the adsorbed HNO_3, calcium sulfate ($CaSO_4$) particles were exposed to gas phase HNO_3. The IR absorption peaks of adsorbed HNO_3 were observed at 1670, and 1720 cm^{-1}; therefore, we can assign the peaks at

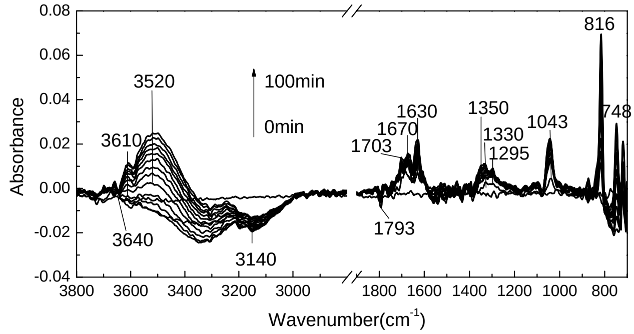

Fig. 1. Typical IR spectra of $CaCO_3$ particles after reaction with NO_2 under dry conditions (RH<10%) at 296 °K and reaction times of 0 to 100 min, NO_2 concentration was 1.22×10^{16} molecule cm^{-3}.

1670 and 1703 cm^{-1} to adsorbed HNO_3, which suggests that HNO_3 was formed when NO_2 reacted with $CaCO_3$.

The peaks at 1630 and 3520 cm^{-1} were assigned to the bending and asymmetric stretching of crystal hydrate water. Compared with the vibration frequencies of the crystallized water in $Ca(NO_3)_2\cdot4H_2O$ at 1640 cm^{-1} and 3490 cm^{-1}, a shift of both peaks occurred, due to the decreased hydrogen bonding. The asymmetric stretching shifted to the higher wave number, and the bending shifted to the lower wave number. The peaks at 3140 and 3330 cm^{-1} were assigned to surface adsorbed water, both peaks decreased as the reaction proceeded until the peaks for crystal hydrate water at 1630 cm^{-1} and 3520 cm^{-1} appeared.

The XPS spectrum of $CaCO_3$ particle that reacted with 1.06×10^{15} molecules cm^{-3} NO_2 for 626 min (Fig. S3, panel a: http://www.atmos-chem-phys.net/10/463/2010/acp-10-463-2010-supplement.pdf) showed the peak of nitrogen of +5 valence at 407.3 eV, confirmed the formation of nitrate. The formation of nitrate was further confirmed by IC analysis of reacted $CaCO_3$ particles (Fig. S3, panel b: http://www.atmos-chem-phys.net/10/463/2010/acp-10-463-2010-supplement.pdf). However, no nitrite was detected with both XPS and IC, this is probably due to the reason that HONO formed in the reaction was released into the gas phase and carried away by N_2.

Figure 2 shows the formation of nitrate on $CaCO_3$ through the reaction of NO_2 as a function of time. The amount of nitrate formed is represented by the integrated absorbance (I_A) of the IR peak area between 1077 and 1013 cm^{-1}. As the reaction proceeded, the nitrate concentration on the calcite surface increased with time and the rate of nitrate formation increased with higher NO_2 concentrations. The nitrate formation process could be divided into three stages: at stage I nitrate concentration on the surface increased linearly with time. This stage lasted about 10 to 20 min, depending on NO_2 concentration. Stage II was the transition stage when the increase of I_A was slowing down, and stage III was

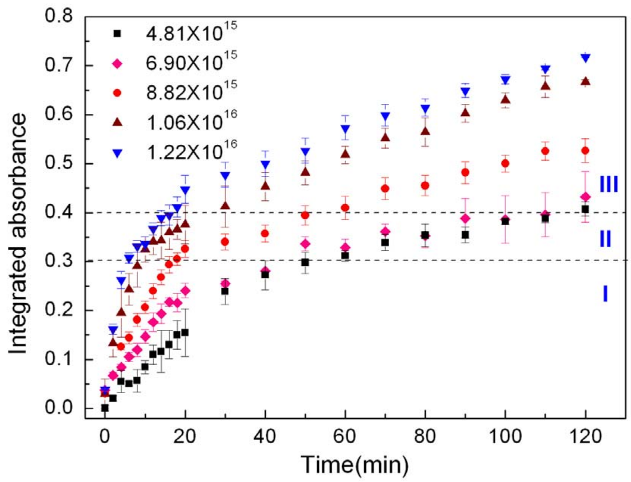

Fig. 2. Nitrate formation as a function of time during the reaction of $CaCO_3$ with NO_2. The nitrate concentration is represented by the integrated absorbance of the peak area between 1077 and 1013 cm^{-1}. The NO_2 concentration was changed from 4.81×10^{15} to 1.22×10^{16} molecule m^{-3}. The data points and the error bars are the average value and the standard deviation of three duplicate experiments.

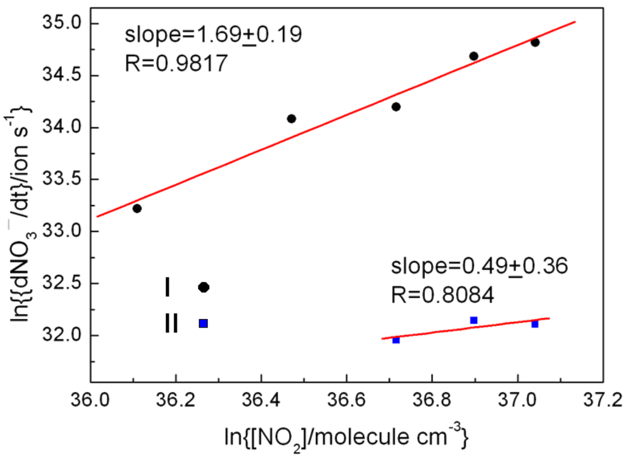

Fig. 3. Double-log curves of nitrate-producing rate versus NO_2 concentration. The data points and error bars are the average values and standard deviations of three replicate experiments. The reaction order was of NO_2 1.69±0.19 in initial stage I (0–10 min), and 0.49±0.36 in transition stage II.

the growth stage when I_A was increasing at a constant rate, smaller than that of stage I.

The amount of nitrate ions formed on the particles $\{NO_3^-\}$ was determined with a linear relationship between I_A in the range of 1073–1013 cm^{-1} and the amount of nitrate determined by ion chromatography $\{NO_3^-\}$:

$$\{NO_3^-\} = f \times I_A \quad (1)$$

The conversion factor f was found to be independent of reaction time and NO_2 concentration as long as the experiment was completed at a stage when the absorption of the nitrate band was still growing. For our study, f was calculated to be 1.89×10^{18} molecules/I_A.

Using f, the formation rate of nitrate $d\{NO_3^-\}/dt$ was calculated, and the reaction order of NO_2 on $CaCO_3$ particles were obtained from the slope of the double-log plots of $d\{NO_3^-\}/dt$ versus NO_2 concentrations (Fig. 3). Using the slope of the initial linear portion (0–10 min) to determine ln{dNO3−}/dt}, the reaction order of NO_2 in stage I was determined as 1.69±0.19 and in stage II 0.49±0.36 in the range of NO_2 concentration in this study.

3.2 Reaction under wet conditions

Experiments of $CaCO_3$ reaction with NO_2 under wet conditions were carried out using non-heat-treated $CaCO_3$ particles at 296 °K with RH=60–71%. Figure 4a shows typical IR spectra of $CaCO_3$ when NO_2 entered the reactor under wet conditions, at reaction times from 0 to 60 min.

The peak at 1048 cm^{-1} was assigned to the symmetric stretching ν_1 of nitrate, the peak at 1344 cm^{-1} to the asymmetric stretching ν_3 of nitrate. The peak at 1251 cm^{-1} was assigned to the asymmetric stretching ν_3 of nitrite. The peak at 1688 cm^{-1} was assigned to the adsorption peak of HNO_3 and the peak at 1636 cm^{-1} to the bending of the surface adsorbed water; the peak at 1472 cm^{-1} appeared in the range of peaks for the asymmetric stretching of carbonate and was assigned to the carbonate vibration peak. Compared to the corresponding peak observed under dry conditions, these peaks had all shifted more or less. We attributed these shifts to the changed environment caused by increased surface adsorbed water under wet conditions.

The peaks at 1525 and 1540 cm^{-1} were in the range of asymmetric stretching of bicarbonate and were assigned to the bicarbonate vibration peaks (Al-Hosney and Grassian, 2004; Al-Abadleh et al., 2005). Negative peaks at 1472, 1525, and 1540 cm^{-1} were similar to the negative peaks from the reaction of HNO_3 with $CaCO_3$ (Fig. S4: http://www.atmos-chem-phys.net/10/463/2010/acp-10-463-2010-supplement.pdf). This indicated that the intermediate products HCO_3^- and H_2CO_3 were formed during the reaction of NO_2 with $CaCO_3$. The result is consistent with the findings of (Al-Hosney and Grassian, 2004) that H_2CO_3 was the intermediate product when HNO_3, SO_2, HCOOH and CH_3COOH reacted with $CaCO_3$.

The formation of nitrate and nitrite was further confirmed by the XPS spectrum of $CaCO_3$ particles reacting with 1.06×10^{15} molecules cm^{-3} of NO_2 for 30 min at RH=80±2%, which demonstrated distinctly the existence of N of +5 valence and +3 valence as shown in Fig. 5a, and the clear formation of nitrate and nitrite shown in IC chromatogram of Fig. 5b.

Figure 4a shows the IR spectrum of H_2O (3500 cm^{-1}), nitrate (1048 cm^{-1}), nitrite (1248 cm^{-1}), and $CaCO_3$ (1472,

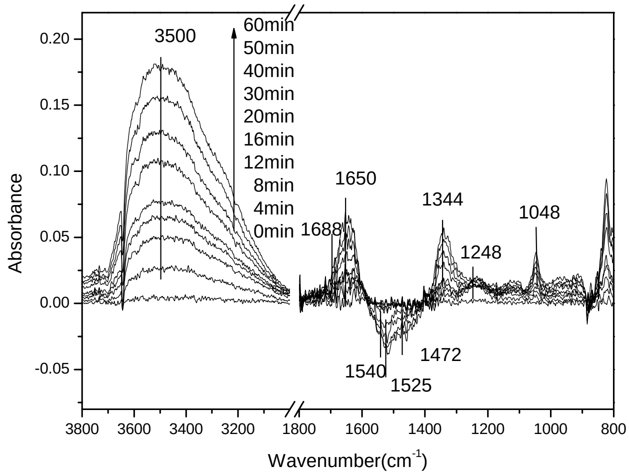

(a)

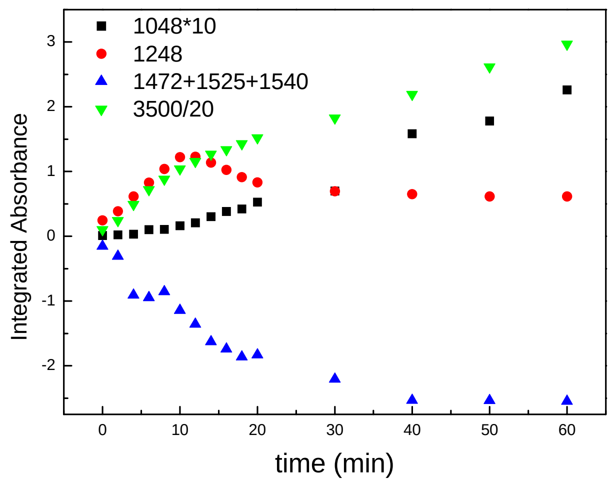

(b)

Fig. 4. **(a)** IR spectrum of H_2O (3500 cm^{-1}), nitrate (1048 cm^{-1}), nitrite (1248 cm^{-1}), and $CaCO_3$ (1472, 1525, 1540 cm^{-1}) during the $CaCO_3$ particles reaction with 1.06×10^{16} molecules cm^{-3} NO_2 from 0 to 60 min, with RH=60–71%. **(b)** Change in integrated absorbance of 1048 cm^{-1} for nitrate, 1248 cm^{-1} for nitrite, 1472+1525+1540 cm^{-1} for $CaCO_3$, and 3500 cm^{-1} for H_2O.

1525, 1540 cm^{-1}) during the $CaCO_3$ particles reaction with 1.06×10^{16} molecules cm^{-3} NO_2 from 0 to 60 min, with RH=60–71%.

Figure 4b shows the time curves of integrated absorbance of 1048 cm^{-1} for nitrate, 1248 cm^{-1} for nitrite, 1472+1525+1540 cm^{-1} for $CaCO_3$, and 3500 cm^{-1} for H_2O. During the first 10 min it shows clearly the fast increases in the concentrations of H_2O and nitrites, and the fast decrease in $CaCO_3$, while the absorbance of nitrate increase gradually. After 10 min, the nitrite concentration started to decrease, while the increase in the concentrations of H_2O and nitrate, and the decrease in the concentrations of $CaCO_3$ maintained at relative slow and steady rates. It was inferred that the increase of adsorbed nitric acid caused the release of nitrite in the form of gaseous HONO which led to the decrease of the concentration of nitrite ions.

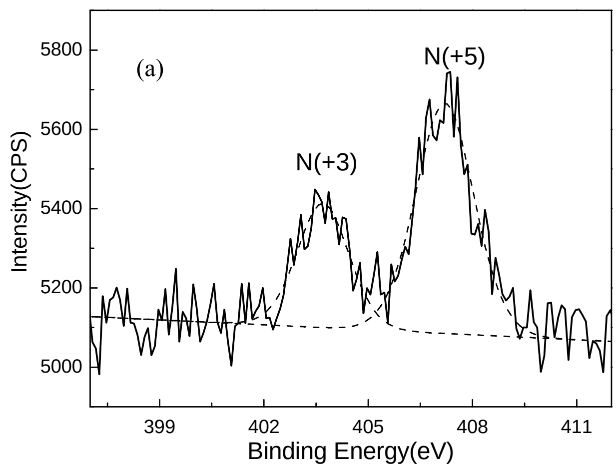

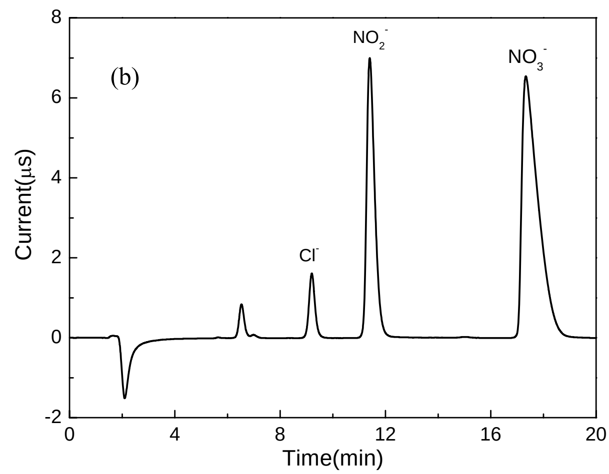

Fig. 5. XPS spectrum **(a)** and IC chromatogram **(b)** analysis of $CaCO_3$ particles after reaction with 1.06×10^{16} molecules cm^{-3} of NO_2 at RH=80±2% for 30 min. The dashed line in (a) was the Lorentzian peak fit.

Figure 6 shows the nitrate formation as a function of time at different NO_2 concentrations during the reaction of $CaCO_3$ with NO_2 under wet conditions (RH=60–71%). The integrated absorbance was in the range of 1077 and 1013 cm^{-1}. Unlike the reaction under dry conditions, under wet conditions, the nitrate on the $CaCO_3$ surface increased linearly with time but did not become saturated during the experimental period, and the nitrate formation rate increased with increasing NO_2 concentration.

Using the conversion factor $f=1.89\times10^{18}$ molecules/I_A, the integrated absorbance of the nitrate peak in the range of 1077 and 1013 cm^{-1} was converted to the number of nitrate ions formed on $CaCO_3$ particle surface $\{NO_3^-\}$. The reaction order of NO_2 was obtained from the slope of the double-log

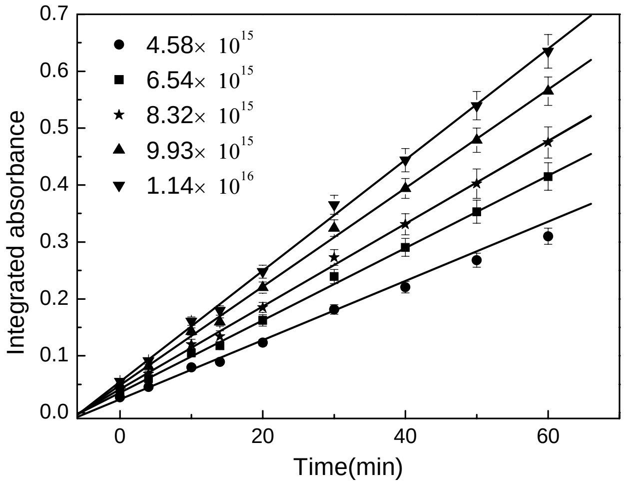

Fig. 6. Nitrate formation as a function of time during the reaction of $CaCO_3$ with NO_2 at 60–71% RH. The nitrate concentration is represented by the integrated absorbance of the peak area between 1077 and 1013 cm^{-1}. The NO_2 concentration was changed from 4.58×10^{15} to 1.14×10^{16} molecule m^{-3}. The data points and the error bars are the average value and the standard deviation of three duplicate experiments.

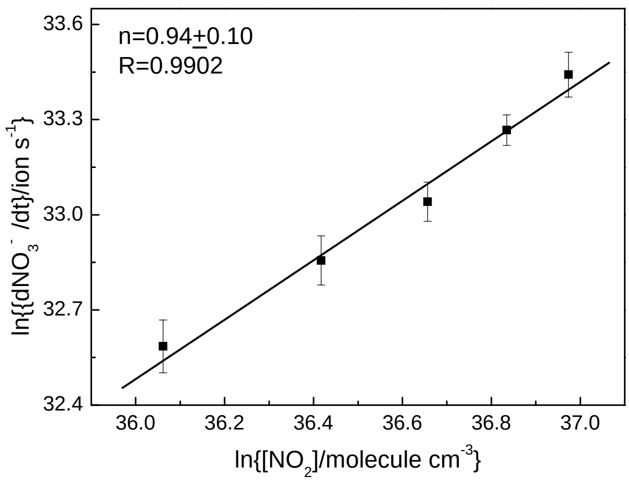

Fig. 7. Double-log plot of the nitrate formation rate versus the NO_2 concentration. The reaction was at 296 °K and RH=66±2%. The data points and error bars are the average values and standard deviations of two or three replicate experiments.

plot of the nitrate formation rate $d\{NO_3^-\}$/dt versus the NO_2 concentration (Fig. 7). Slope of the curve was 0.94±0.10, this means that under wet conditions, the NO_2 reaction on $CaCO_3$ particles is first order with respect to NO_2 in the NO_2 concentration range of this study.

Here we assumed that the conversion factor f is the same under both wet and dry conditions, this assumption may cause bias in NO_3^- concentrations, because the spectra under dry and wet conditions could be different, which may influence the conversion factor f. We tried our best to reduce this possible bias: (1) the peak we used for quantitative analysis was the symmetric stretching of nitrate ν_1 (with an integration range of 1073–1013 cm^{-1}), where there is no interference from other peaks. When changed from dry to wet conditions, the peak maintained the same shape and shifted slightly, from 1043 cm^{-1} to 1048 cm^{-1}; (2) the conversion factor is also related to the sample property such as sample stack density and particle size; in our experiment the same sample preparation procedure were used for both the dry and wet experiment this should minimize the difference caused by sample property. In a future study, the relationship of the conversion factor and RH should be verified.

3.3 The influence of water vapor

Calcite is the main form of $CaCO_3$ in the environment and its (1014) crystal plane has the lowest energy state (de Leeuw and Parker, 1998). Both laboratory and computer modeling studies have demonstrated that at certain relative humidity, a hydrated layer on $CaCO_3$ could be dissociated by oxygen vacancy to form stable −OH that remained surface-bound even in a high vacuum (Stipp et al., 1996; McCoy and LaFemina, 1997; de Leeuw and Parker, 1998). The results of Kuriyavar et al. (2000) and Stipp (1999) demonstrated that the dissociation of water could produce surface hydroxyl on $CaCO_3$ surfaces. Species including H^+, OH^+, HCO_3^-, $Ca(OH)^-$, and $Ca(HCO_3)^-$ can exist on the surfaces of calcite and alter its surface properties (Thompson and Pownall, 1989). XPS analysis of our $CaCO_3$ particle sample showed two peaks of O1s at 531.3 eV and 533.1 eV (Fig. S5: http://www.atmos-chem-phys.net/10/463/2010/acp-10-463-2010-supplement.pdf), corresponding to the oxygen atoms of $CaCO_3$ and −Ca(OH) (Stipp, 1999). The oxygen atoms of −Ca(OH) accounted for 3.4–3.6% of the total number of atoms, and the oxygen atom ratio of Ca(OH):$CaCO_3$ was 7.3:100. The presence of −Ca(OH) implied that water can have a major effect on the $CaCO_3$ surface properties. Therefore, understanding water adsorption on surfaces of $CaCO_3$ particles is very important.

From the IR spectra of the $CaCO_3$ particle samples, we integrated the area of the stretching vibration of −OH from 3644 to 2983 cm^{-1} and plotted it as a function of RH at 296 K (Fig. S6, left axis: http://www.atmos-chem-phys.net/10/463/2010/acp-10-463-2010-supplement.pdf), it demonstrated that the proportion of surface bound water increased with RH. The NO_3^- formation rate on the $CaCO_3$ particle samples can be expressed as:

$$d\{NO_3^-\}/dt = k\{CaCO_3\}^m[H_2O]^q[NO_2]^n \quad (2)$$

where {} denotes the concentration of surface species (e.g. nitrate ions and active site on $CaCO_3$), [] denotes the concentration of species in gas phase, and m, n, and q are the reaction order for $CaCO_3$, NO_2 and H_2O, respectively. At the initial stage of the reaction, the number of NO_3^- ions formed on the surface of $CaCO_3$ is small compared to the surface active site, $\{CaCO_3\}$ can be considered constant.

The reaction rate of NO_2 on $CaCO_3$ particle was investigated as a function of RH (Fig. 8a). The nitrate formation rate decreases initially with RH and then increases slightly with the increasing RH.

The reaction order of H_2O was obtained from slope double-log curve of the NO_3^- formation rate versus the water concentration at a constant NO_2 concentration (Fig. 8b). The reaction order of $H_2O(g)$ was -0.44 with RH<50%, and 0.20 with RH>50%.

The change of nitrate formation rate with RH indicates the influence of water vapor on the reaction mechanism of NO_2 on $CaCO_3$ particles. At low RH, the surface −OH determines the reaction rate and water competes with NO_2 for the active sites (surface −OH), and the uptake coefficient decreases with the increase in RH.

As RH increases, water starts to condense on the surface to form micro-puddles of water (Krueger et al., 2005), and gas-liquid reaction of NO_2 with condensed water may become feasible. With RH high enough (>52% in our experiment), the gas-liquid reaction of NO_2 with condensed water may become rate limiting, and the nitrate formation rate increases with RH. This is consistent with the observation that at low RH, the formation of the active site on the surface of the $CaCO_3$, e.g. −OH, involved the adsorbed water, which can alter the reactivity of the particle surface (Elam et al., 1998; Hass et al., 1998; Eng et al., 2000; Hass et al., 2000). Water could easily adsorb onto the surface −OH, and compete with the adsorption of NO_2 (Stumm, 1992). At high RH, as more condensed water forms on the surface of $CaCO_3$, the reaction on the calcite surface can change from gas-solid to gas-liquid reaction. Thus, water plays an important role in determining the mechanism of the heterogeneous reactions of NO_2 with $CaCO_3$. Details of the mechanism will be discussed below.

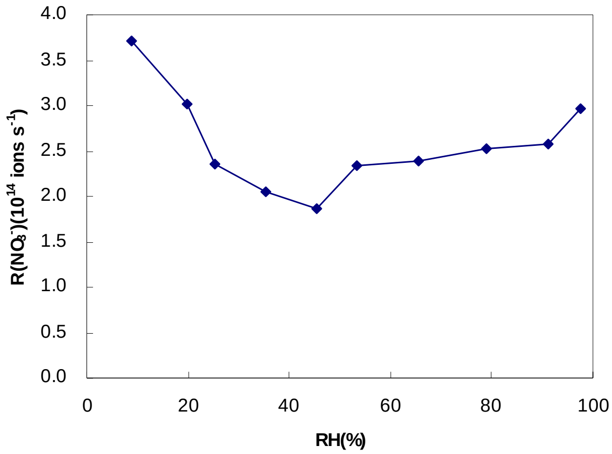

(a)

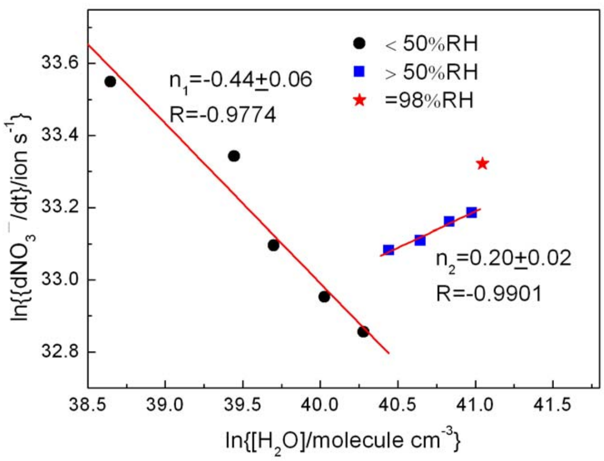

(b)

Fig. 8. Nitrate formation rate during the reaction of $CaCO_3$ with NO_2 **(a)** and double-log curve of NO_3^- formation rate versus $[H_2O]$ **(b)** at different RH and a constant NO_2 concentration of 6.88×10^{15} molecules cm^{-3}.

3.4 Uptake coefficient

The reactive uptake coefficient or reaction probability, γ, is defined as the ratio of the reactive gas-surface collision rate to the total gas-surface collision rate. The reactive uptake coefficient of NO_2 by the surface of the $CaCO_3$ particles is

$$\gamma=\frac{dN(NO_2)/dt}{Z} \tag{3}$$

$$Z=\frac{1}{4}A\omega\, n \tag{4}$$

where $N(NO_2)$ is the number of reactive NO_2 collisions with the surface, Z is the total gas-surface collision rate of NO_2 on the surface of $CaCO_3$, A is the surface area of $CaCO_3$ particles (BET surface area was used here), ω is the mean speed of the gas molecule, and n is the concentration of gas phase species. The rate of reactive collisions can be obtained from the formation rate of nitrate d{NO3−}/dt, the reactive uptake coefficient then becomes:

$$\gamma=\frac{d\left\{NO_3^-\right\}/dt}{Z} \tag{5}$$

Previous studies show that the reaction of NO_2 with particles was through N_2O_4 (Finlayson-Pitts et al., 2003), then the reactive NO_2 loss rate in the gas phase is twice of the nitrate formation rate.

The nitrate formation rate $d\{NO_3^-\}/dt$ could be calculated from the curve of nitrate formation as a function of time, and the nitrate formation rate in the initial stage of the reaction

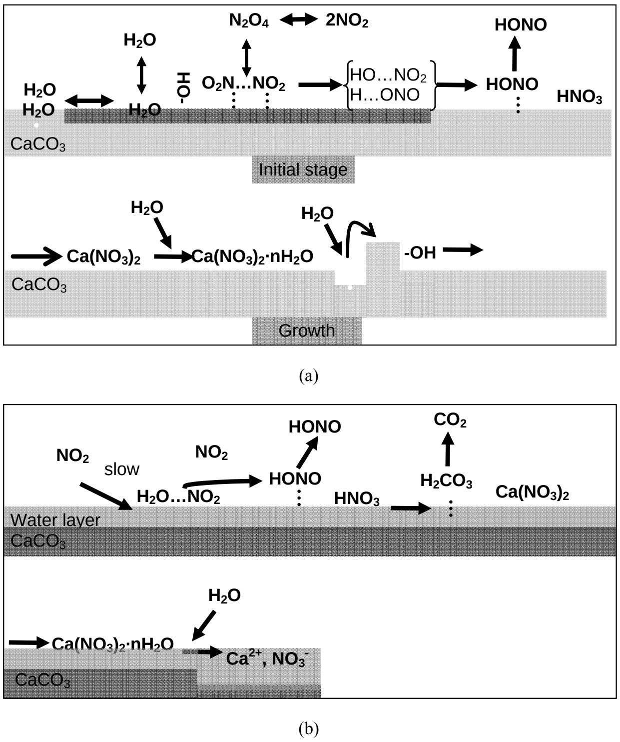

Fig. 9. Schematics of the mechanism of NO_2 reaction on the surface of $CaCO_3$ particles under **(a)** dry and **(b)** wet conditions.

was used for calculating the initial uptake coefficient γ_0. Table 1 lists the initial uptake coefficient of NO_2 on $CaCO_3$ particles under both dry (RH<10%) and wet (RH=60–71%) conditions. The initial uptake coefficient under dry conditions was $(4.25\pm1.18)\times10^{-9}$, while under wet conditions, it is slightly lower, with a value of $(2.54\pm0.13)\times10^{-9}$. These values are at the same level as those reported by Boerensen et al. (2000) about the reactive uptake coefficient of NO_2 on Al_2O_3.

4 Discussion

We conclude from the above results that water vapor has an important influence on the heterogeneous reaction mechanism of NO_2 with $CaCO_3$. The reaction mechanism is different under dry and wet conditions. Under dry conditions, −OH is produced on the calcite surface via the dissociation of water by oxygen vacancy and this seems to be the rate determining factor for the reaction. As RH increases and more water condenses on $CaCO_3$ surface, surface condensed water participates in the reaction. We discuss the reaction mechanisms for both of these two conditions below.

Table 1. Initial uptake coefficient of NO_2 on $CaCO_3$ particles under dry and wet conditions. The RH was measured at 296 K.

replicate time	$[NO_2]$ (10^{15} molecule cm^{-3})	$\gamma_0\pm2\,\sigma$ (10^{-9})	RH (%)
14	6.90∼16.84	4.25±1.18	dry
5	4.58∼11.40	2.54±0.13	60-71

4.1 Mechanism under dry conditions

Under dry conditions, the reaction mechanism proceeded as shown in Fig. 9a. At low RH, there was still some water vapor remaining and the surface adsorbed water on the $CaCO_3$ surface equilibrated with water vapor, as shown in Reaction (R1):

$$H_2O(g) \underset{k_{-1}}{\overset{k_1}{\rightleftharpoons}} H_2O(a) \tag{R1}$$

Surface-adsorbed water existed on the $CaCO_3$ surface despite heating at 623 °K for 2 h. The adsorbed water on the $CaCO_3$ surface was dissociated by an oxygen vacancy site(O) to form the active site S·(OH)H that was stable even at high temperature and high vacuum:

$$\text{site(O)} + H_2O(a) \xrightarrow{k_2} S\cdot(OH)H \tag{R2}$$

Finlayson-Pitts et al. (2003) found NO_2 was likely to form nitrogen dioxide dimers (nitrogen tetroxide, N_2O_4) at high concentrations,

$$2NO_2(g) \underset{k_{-3}}{\overset{k_3}{\rightleftharpoons}} N_2O_4(g) \tag{R3}$$

NO_2 was in equilibrium with N_2O_4 in the gas phase,

$$[N_2O_4]=\frac{k_3}{k_{-3}}[NO_2]^2 = K_3[NO_2]^2 \tag{6}$$

then N_2O_4 was adsorbed to the particle surface:

$$N_2O_4(g) \underset{k_{-4}}{\overset{k_4}{\rightleftharpoons}} N_2O_4(a) \tag{R4}$$

N_2O_4 reacted with the surface active site forming adsorbed nitric acid HNO_3 and nitrous acid HONO, as illustrated in Reaction (R5):

$$N_2O_4(a) + S\cdot(OH)H \xrightarrow{k_5} \text{site(O)} \tag{R5}$$
$$-HNO_3(a)+HONO(g)$$

$$\frac{d\{HNO_3\}}{dt} = k_5\{N_2O_4\}\{S\cdot(OH)H\} \tag{7}$$

Compared to "sticky" HNO_3, HONO was unlikely to adsorb onto surface, but rather being released into the gas phase (Goodman et al., 1999; Borensen et al., 2000). Although we could not detect gas phase HONO, we did detect adsorbed HNO_3 with DRIFTS.

No adsorbed N_2O_4 was observed on the particle surface, suggesting N_2O_4 could be treated as an intermediate in the reaction:

$$\frac{d\{N_2O_4\}}{dt} = k_4[N_2O_4] - k_{-4}\{N_2O_4\} - k_5\{N_2O_4\}\{S\cdot(OH)H\} = 0 \tag{8}$$

Assuming the HNO_3 formed was quickly converted to NO_3^- on the surface of $CaCO_3$. Then

$$\frac{d\{NO_3^-\}}{dt} = \frac{d\{HNO_3\}}{dt} = k_5\{N_2O_4\}\{S\cdot(OH)H\} \tag{9}$$

Combining Eqs. (6), (7), (8), and (9), one can get

$$\frac{d\{NO_3^-\}}{dt} = \frac{k_4k_5K_3[NO_2]^2\{S\cdot(OH)H\}}{k_{-4}+k_5\{S\cdot(OH)H\}} \tag{10}$$

Equation (10) shows that, at the initial stage of the reaction, the amount of surface active sites was relatively large and formation of HNO_3 on the $CaCO_3$ surface was a second-order reaction with respect to NO_2. This is consistent with the measured reaction order of 1.69 ± 0.19 as illustrated in Fig. 3, even though the NO_2 concentration range is small due to the limits from experiment conditions.

Underwood et al. (1999, 2001) suggested that under dry conditions NO_2 might first react to form a surface nitrite, which was then oxidized by NO_2. However, in our experiment, we did not detected surface nitrite under dry conditions, the reason for this is likely the high NO_2 concentration used in our experiment compared to the studies Underwood et al. (1999, 2001), and this confirms the mechanism involving the reaction of N_2O_4 at the high NO_2 pressure of the present study.

Based on the mechanism discussed above, under dry conditions, surface nitrate should increase exponentially and reach saturation due to the depletion of surface reactive sites; which is consistent with the experimental observation at the stage I and II (Fig. 2). However, at the third stage, the nitrate was found grow continuously instead of leveling off gradually. This indicates the rate law may not work at the stage III. Other reaction process, such as the reaction of NO_2 with water in newly formed $Ca(NO_3)_2$ may contribute to the continuous formation of surface nitrate at this stage. Further study is needed to understand the mechanism at stage III.

4.2 Mechanism under wet conditions

Here, the wet conditions refer to the conditions when RH>52%. The reaction mechanism under wet conditions was illustrated by the general scheme in Fig. 9b. NO_2 was adsorbed on $CaCO_3$ to form adsorbed NO_2(a):

$$NO_2(g) \underset{k_{-6}}{\overset{k_6}{\rightleftharpoons}} NO_2(a) \tag{R6}$$

Previous studies have demonstrated that the disproportionation reaction of NO_2 with surface adsorbed water was a first-order reaction, with the adsorption of NO_2 being the rate-limiting step (Svensson et al., 1987; Jenkin et al., 1988). The nitrite and nitrate formed on the particle surface was attributed to the reaction of surface-adsorbed water with NO_2; i.e., adsorbed NO_2(a) reacted with condensed water H_2O(a) to form adsorbed HNO_3(a) and gaseous HONO(g).

$$H_2O(a)+2\,NO_2(a) \xrightarrow{k_7} HNO_3(a)+HONO(g) \tag{R7}$$

At the initial stage, HONO dissolved in adsorbed water to form nitrite. As the concentration of HNO_3(a) increased, the surface pH decreased and nitrite escaped from the surface as gaseous HONO. Meanwhile, HNO_3(a) reacted with $CaCO_3$ to form H_2CO_3 and $Ca(NO_3)_2$ (Al-Hosney and Grassian, 2004).

$$2HNO_3(a)+CaCO_3(s) \xrightarrow{k_8} Ca(NO_3)_2(s)+H_2CO_3(a) \tag{R8}$$

Afterwards, H_2CO_3 decomposed in adsorbed water to form H_2O and CO_2, resulting in the decrease of HCO_3^- and CO_3^{2-} on the surface.

$$H_2CO_3(a) \longrightarrow H_2O(g)+CO_2(g) \tag{R9}$$

$Ca(NO_3)_2$ has strong hygroscopic property and the $Ca(NO_3)_2$ particles were in the form of solution droplets at RH>10% (Liu et al., 2008b), this caused the broadened peak for adsorbed water in the IR spectrum.

$$Ca(NO_3)_2(s)+nH_2O(a) \rightleftharpoons Ca(NO_3)_2\cdot nH_2O \tag{R10}$$

Since the adsorption of NO_2 was the rate-limiting step and HNO_3(a) was the intermediate product, the rate of nitrate formation in the presence of excess surface water could be expressed as the following.

$$\frac{d\{NO_3^-\}}{dt} = \frac{1}{2}k_6[NO_2] \tag{11}$$

Equation (11) shows the surface nitrate formation with respect to NO_2 as a first order reaction; this is consistent with the experimental result of 0.94 ± 0.10.

Under wet conditions, N_2O_4 could also be involved in the reaction of NO_2 with the condensed phase water, and the reaction order for loss of NO_2 was reported as 1.6 ± 0.2 (Finlayson-Pitts et al., 2003). Lee and Schwartz (1981) reported that for the NO_2 reaction with liquid water, the apparent reaction order in NO_2 could change from 1 to 2, depending on the reaction regime, such as phase mixed, convective mass transport, and diffusive mass transport. The presence of N_2O_4 in solution is also a factor determining the apparent reaction order in NO_2. Under convective mass transport conditions, the NO_2 reaction order should be 1. Our experiments found that the NO_2 reaction order is 0.94±0.10. However, the surface/volume ratio in our experimental was about $10^6\,m^{-1}$, this is much higher than the 100–800 m^{-1} interfacial area per unit liquid volume in the study of Lee and Schwartz (1981). Thus the reaction under our experimental conditions is unlikely limited by the convective mass transport; further analysis is needed to explain the reason for reaction order of 0.94±0.10 in NO_2.

In our experiments, the NO_2 concentration range was narrow for reaction order determination: 4.81×10^{15} to 1.22×10^{16} molecule m^{-3} under dry conditions, and 4.58×10^{15} to 1.14×10^{16} molecules m^{-3} under wet conditions. This is unfortunately limited by the current experimental setup. With DRIFTS system the gas concentration can neither be too low due to the detection limit of the instrument nor too high because of the fast nitrate formation in the initial stage of the reaction, which may hinder obtaining exact reaction rate from the kinetic curve. However, this narrow range should not prevent us from discussing the reaction order, as long as we do not extrapolate the results outside the range of NO_2 concentration. Moreover, the correlation coefficient is high in Fig. 3 (R=0.98) which implies the reaction order is reliable within the NO_2 concentration range. If future experimental conditions allowed, one should expand the range of NO_2 concentrations for rate order determination.

4.3 Implications for the troposphere

Under dry conditions (RH<10%), formation of N_2O_4 is the first reaction step. In the troposphere, the NO_2 concentrations are orders of magnitude smaller than that used in our experiments, the N_2O_4 concentrations in the troposphere should be even lower than our experiment conditions, with a γ_0 of $(4.25\pm1.18)\times10^{-9}$, the reaction of NO_2 on $CaCO_3$ under dry conditions may not have important implication in the atmosphere.

Table 1 shows that under dry and wet conditions, γ_0 were varied within a range of $2.5\text{–}4.3\times10^{-9}$, which is narrower than we anticipated. At RH>52%, with the increase of water condensed on the surface of $CaCO_3$ particles, the γ_0 of NO_2 on $CaCO_3$ particles calculated using BET surface area could have been underestimated. As significant amount of condensed water could make the surface of $CaCO_3$ particles smoother and less pores, the available surface area for the reaction should be close to the geometric surface area of a cubic shape particle.

When calculating the uptake coefficient, to use which type of surface area depends on the surface properties of the particles. For our experiment, at wet conditions and with significant amount of condensed water on the surface, we should use geometric surface area to calculate γ_0.

Using $0.19\,m^2\,g^{-1}$ as the specific geometric surface area of $CaCO_3$ particle samples, from Table 1 we calculated γ_0 at RH=60–71% to be $(6.56\pm0.34)\times10^{-8}$; this is more than twenty times higher than the value calculated with BET surface area.

The uptake coefficient of HNO_3 on $CaCO_3$ has been measured by many researchers using different methods, it was found to increase with RH (Vlasenko et al., 2006; Liu et al., 2008) and varies from $10^{-5}\sim10^{-4}$ (Goodman et al., 2000; Underwood et al., 2000; Johnson et al., 2005) at 0% RH to 0.01–0.1 at >20% RH. The large variation of the uptake coefficient of HNO_3 on $CaCO_3$ may due to different methods as well as the different surface areas used in calculating uptake coefficient (Fenter et al., 1995; Hanisch and Crowley, 2001). Even considering that NO_2 concentrations in the atmosphere is orders of magnitude higher than that of HNO_3, our experimental results suggest that the reaction of NO_2 on $CaCO_3$ particle is unable to compete with that of HNO_3 in the atmosphere.

However, under wet conditions or RH>52%, in order to obtain reliable uptake coefficients, one needs to carefully choose the type the surface area and determine it accurately. Moreover, under wet conditions, the IR, XPS, and IC evidences for the formation of nitrite and its subsequent decrease on $CaCO_3$ particle suggests the reaction of NO_2 with $CaCO_3$ could be a source of HONO in the atmosphere.

5 Conclusions

The heterogeneous reaction of NO_2 with $CaCO_3$ under dry and wet conditions produced nitrate. Under wet conditions, nitrite formation was observed with IR, XPS, and IC, indicating the reaction of NO_2 on the $CaCO_3$ surface probably produced nitrous acid (HONO). Relative humidity (RH) influenced both the initial uptake coefficient and the reaction mechanism. The initial uptake coefficient of NO_2 on $CaCO_3$ particles γ_0 was found to change with increasing relative humidity. Using BET surface area, γ_0 under dry conditions (RH∼0%) was determined to be $(4.25\pm1.18)\times10^{-9}$, while under "wet" conditions (RH=60–71%), it was slightly lower, with a value of $(2.54\pm0.13)\times10^{-9}$. Our results show that relative humidity had a major influence on the surface properties of $CaCO_3$ particles by not only influencing the initial uptake coefficient but also by changing the reaction mechanism. At low RH, surface −OH produced via the dissociation of surface-adsorbed water by an oxygen vacancy on the $CaCO_3$ surface was the rate determining factor in the reaction. The reaction was second order in NO_2. As RH increases, water starts to condense on the surface and the gas-liquid reaction of NO_2 with the condensed water begins. With high enough RH (>52% in our experiment), the gas-liquid reaction of NO_2 with condensed water becomes dominant, producing HNO_3 and HONO. At this stage, the reaction appeared to be first order in NO_2.

At high RH, condensed water could make the surface smoother with less pores, other than the BET surface area, the geometric surface area should be used to calculate γ_0. Using $0.19\,m^2\,g^{-1}$ as the specific geometric surface area of $CaCO_3$ particle samples, we calculated γ_0 at RH=60–71% to be $(6.56\pm0.34)\times10^{-8}$; this is more than twenty times higher than that under dry conditions. Moreover, $CaCO_3$ is alkaline and can react with NO_2 to form calcium nitrate which has strong hygroscopicity and could deliquesce at RH$>$10%. This will help exposing $CaCO_3$ to NO_2, until $CaCO_3$ is fully reacted.

The uptake coefficient of HNO_3 on $CaCO_3$ ranged from 10^{-4} to 0.1, depending on RH. Our results show that the heterogeneous reaction of NO_2 on $CaCO_3$ is unable to compete with that of HNO_3 in producing calcium nitrate on mineral aerosol in the atmosphere. However, the NO_2 reaction with water adsorbed on $CaCO_3$ could be a source of HONO in the atmosphere. Further efforts to detect HONO formed in the reaction of NO_2 on $CaCO_3$ particles are necessary.

Acknowledgements. This work was supported by the National Basic Research Priorities Program (Grant No. 2002CB410802) and National Natural Science Foundation of China (Grant No. 40490265, 20637020).

Edited by: M. Ammann

References

Al-Abadleh, H. A., Al-Hosney, H. A., and Grassian, V. H.: Oxide and carbonate surfaces as environmental interfaces: the importance of water in surface composition and surface reactivity, J. Mol. Catal. A-Chem., 228, 47–54, 2005.

Al-Hosney, H. A. and Grassian, V. H.: Carbonic acid: An important intermediate in the surface chemistry of calcium carbonate, J. Am. Chem. Soc., 126, 8068–8069, 2004.

Boerensen, C., Kirchner, U., Scheer, V., Vogt, R., and Zellner, R.: Mechanism and kinetics of the reactions of NO_2 or HNO_3 with alumina as a mineral dust model compound, J. Phys. Chem. A, 104, 5036–5045, 2000.

Carmichael, G. R., Zhang, Y., Chen, L. L., Hong, M. S., and Ueda, H.: Seasonal variation of aerosol composition at Cheju Island, Korea, Atmos. Environ., 30, 2407–2416, 1996.

Chen, L. Q.: Long range atmospheric transport of China desert aerosol to north Pacific Ocean, Acta Oceanol. Sin., 7, 554–560, 1985.

de Leeuw, N. H. and Parker, S. C.: Surface structure and morphology of calcium carbonate polymorphs calcite, aragonite, and vaterite: an atomistic approach, J. Phys. Chem. B, 102, 2914–2922, 1998.

Dentener, F. J., Carmichael, G. R., Zhang, Y., Lelieveld, J., and Crutzen, P. J.: Role of mineral aerosol as a reactive surface in the global troposphere, J. Geophys. Res.-Atmos., 101, 22869–22889, 1996.

Elam, J. W., Nelson, C. E., Cameron, M. A., Tolbert, M. A., and George, S. M.: Adsorption of H_2O on a single-crystal alpha-Al_2O_3(0001) surface, J. Phys. Chem. B, 102, 7008–7015, 1998.

Eng, P. J., Trainor, T. P., Brown Jr., G. E., Waychunas, G. A., Newville, M., Sutton, S. R., and Rivers, M. L.: Structure of the hydrated alpha-Al_2O_3 (0001) surface, Science, 288, 1029–1033, 2000.

Fenter, F. F., Caloz, F., and Rossi, M. J.: Experimental-Evidence for the Efficient Dry Deposition of Nitric-Acid on Calcite, Atmos. Environ., 29, 3365–3372, 1995.

Finlayson-Pitts, B. J., Wingen, L. M., Sumner, A. L., Syomin, D., and Ramazan, K. A.: The heterogeneous hydrolysis of NO_2 in laboratory systems and in outdoor and indoor atmospheres: An integrated mechanism, Phys. Chem. Chem. Phys., 5, 223–242, 2003.

Goodman, A. L.: A spectroscopic study of heterogeneous reactions of nitrogen oxides and sulfur oxides on solid particles of atmospheric relevance, Chemistry Department, The University of Iowa, Iowa, 276, 2000.

Goodman, A. L., Underwood, G. M., and Grassian, V. H.: Heterogeneous Reaction of NO_2: Characterization of Gas-Phase and Adsorbed Products from the Reaction, $2NO_2(g)+H_2O(a)$f $HONO(g)+HNO_3(a)$ on Hydrated Silica Particles, J. Phys. Chem. A, 103, 7217–7223, 1999.

Goodman, A. L., Underwood, G. M., and Grassian, V. H.: A laboratory study of the heterogeneous reaction of nitric acid on calcium carbonate particles, J. Geophys. Res.-Atmos., 105, 29053–29064, 2000.

Hanisch, F. and Crowley, J. N.: Heterogeneous reactivity of gaseous nitric acid on Al_2O_3, $CaCO_3$, and atmospheric dust samples: A Knudsen cell study, J. Phys. Chem. A, 105, 3096–3106, 2001.

Hass, K. C., Schneider, W. F., Curioni, A., and Andreoni, W.: The chemistry of water on alumina surfaces: Reaction dynamics from first principles, Science, 282, 265–268, 1998.

Hass, K. C., Schneider, W. F., Curioni, A., and Andreoni, W.: First-principles molecular dynamics simulations of H_2O on alpha-Al_2O_3(0001), J. Phys. Chem. B, 104, 5527–5540, 2000.

Jenkin, M. E., Cox, R. A., and Williams, D. J.: Laboratory Studies of the kinetics of formation of nitrous-acid from the thermal-reaction of nitrogen-dioxide and water-vapor, Atmos. Environ., 22, 487–498, 1988.

Johnson, E. R., Sciegienka, J., Carlos-Cuellar, S., and Grassian, V. H.: Heterogeneous Uptake of Gaseous Nitric Acid on Dolomite ($CaMg(CO_3)_2$) and Calcite ($CaCO_3$) Particles: A Knudsen Cell Study Using Multiple, Single, and Fractional Particle Layers, J. Phys. Chem. A, 109, 6901–6911, 2005.

Jonas, P. R., Charlson, R. J., Rodhe, H., Anderson, T. L., Andreae, M. O., Dutton, E., Graf, H., Fouquart, Y., Grassl, H., Heintzenberg, J., Hobbs, P. V., Hofmann, D., Hubert, B., et al.: Aerosols, in Climate Change 1994: Radiative Forcing of Climate Change, edited by: Houghton, J. T., Meira Filho, L. G., Bruce, J., Lee, H., Callander, B. A., Haites, E., Harris, N., and Maskell, K., Cambridge University Press, Cambridge, UK, 127–162, 1995.

Krueger, B. J., Ross, J. L., and Grassian, V. H.: Formation of microcrystals, micropuddles, and other spatial inhomogenieties in surface reactions under ambient conditions: An atomic force microscopy study of water and nitric acid adsorption on MgO(100) and $CaCO_3$(1014), Langmuir, 21, 8793–8801, 2005.

Krueger, B. J., Grassian, V. H., Iedema, M. J., Cowin, J. P., and Laskin, A.: Probing heterogeneous chemistry of individual atmospheric particles using scanning electron microscopy and energy-dispersive X-ray analysis, Anal. Chem., 75, 5170–5179, 2003a.

Krueger, B. J., Grassian, V. H., Laskin, A., and Cowin, J. P.: The transformation of solid atmospheric particles into liquid droplets through heterogeneous chemistry: Laboratory insights into the processing of calcium containing mineral dust aerosol in the troposphere, Geophys. Res. Lett., 30, 1148, doi:10.1029/2002GL016563, 2003b.

Kuriyavar, S. I., Vetrivel, R., Hegde, S. G., Ramaswamy, A. V., Chakrabarty, D., and Mahapatra, S.: Insights into the formation of hydroxyl ions in calcium carbonate: temperature dependent FTIR and molecular modelling studies, J. Mater. Chem., 10, 1835–1840, 2000.

Lee, Y. N. and Schwartz, S. E.: Reaction kinetics of nitrogen dioxide with liquid water at low partial pressure, J. Phys. Chem., 85, 840–848, 1981.

Li, H. J., Zhu, T., Ding, J., Chen, Q., and Xu, B. Y.: Heterogeneous reaction of NO_2 on the surface of NaCl particles, Sci. China Ser. B, 49, 371–378, 2006.

Liu, Y., Gibson, E. R., Cain, J. P., Wang, H., Grassian, V. H., and Laskin A.: Kinetics of Heterogeneous Reaction of $CaCO_3$ Particles with Gaseous HNO_3 over a Wide Range of Humidity, J. Phys. Chem. A, 112, 1561–1571, 2008a.

Liu, Y. J., Zhu, T., Zhao, D. F., and Zhang, Z. F.: Investigation of the hygroscopic properties of $Ca(NO_3)_2$ and internally mixed $Ca(NO_3)_2/CaCO_3$ particles by micro-Raman spectrometry, Atmos. Chem. Phys., 8, 7205–7215, 2008, http://www.atmos-chem-phys.net/8/7205/2008/.

McCoy, J. M. and LaFemina, J. P.: Kinetic Monte Carlo investigation of pit formation at the $CaCO_3$(10(1)over-bar4) surface-water interface, Surf. Sci., 373, 288–299, 1997.

Nakamoto, K.: Infrared and Raman Spectra of Inorganic and Coordination Compounds Part A, New York, John Wiley & Sons, 1997.

Okada, K., Qin, Y., and Kai, K.: Elemental composition and mixing properties of atmospheric mineral particles collected in Hohhot, China, Atmos. Res., 73, 45–67, 2005.

Quan, H.: Discussion of the transport route of dust storm and loess aerosol from Northwest China at the high altitude, Environ. Sci., 14, 60–65, 1993.

Song, C. H. and Carmichael, G. R.: Gas-particle partitioning of nitric acid modulated by alkaline aerosol, J. Atmos. Chem., 40, 1–22, 2001.

Song, C. H., Maxwell-Meier, K., Weber, R. J., Kapustin, V., and Clarke, A.: Dust composition and mixing state inferred from airborne composition measurements during ACE-Asia C130 Flight #6, Atmos. Environ., 39, 359–369, 2005.

Stipp, S. L. S., Gutmannsbauer, W., and Lehmann, T.: The dynamic nature of calcite surfaces in air, Am. Mineral., 81, 1–8, 1996.

Stipp, S. L. S.: Toward a conceptual model of the calcite surface: Hydration, hydrolysis, and surface potential, Geochim. Cosmochim. Ac., 63, 3121–3131, 1999.

Stumm, W.: Chemistry of the solid-water interface: processes at the mineral-water and particle-water interface in natural systems, New York, John Wiley & Sons, 1992.

Sullivan, R. C., Guazzotti, S. A., Sodeman, D. A., and Prather, K. A.: Direct observations of the atmospheric processing of Asian mineral dust, Atmos. Chem. Phys., 7, 1213–1236, 2007, http://www.atmos-chem-phys.net/7/1213/2007/.

Svensson, R., Ljungstrom, E., and Lindqvist, O.: Kinetics of the Reaction between Nitrogen Dioxide and Water Vapor, Atmos. Environ., 21, 1529–1539, 1987.

Thompson, D. W. and Pownall, P. G.: Surface Electrical-Properties of Calcite, J. Colloid Interf. Sci., 131, 74–82, 1989.

Ullerstam, M., Johnson, M. S., Vogt, R., and Ljungström, E.: DRIFTS and Knudsen cell study of the heterogeneous reactivity of SO_2 and NO_2 on mineral dust, Atmos. Chem. Phys., 3, 2043–2051, 2003, http://www.atmos-chem-phys.net/3/2043/2003/.

Underwood, G. M., Li, P., Usher, C. R., and Grassian, V. H.: Determining accurate kinetic parameters of potentially important heterogeneous atmospheric reactions on solid particle surfaces with a Knudsen cell reactor, J. Phys. Chem. A, 104, 819–829, 2000.

Underwood, G. M., Miller, T. M., and Grassian, V. H.: Transmission FT-IR and Knudsen Cell Study of the Heterogeneous Reactivity of Gaseous Nitrogen Dioxide on Mineral Oxide Particles, J. Phys. Chem. A, 103, 6184–6190, 1999.

Vlasenko, A., Sjogren, S., Weingartner, E., Stemmler, K., Gäggeler, H. W., and Ammann, M.: Effect of humidity on nitric acid uptake to mineral dust aerosol particles, Atmos. Chem. Phys., 6, 2147–2160, 2006, http://www.atmos-chem-phys.net/6/2147/2006/.

Zhang, D. Z., Shi, G. Y., Iwasaka, Y., and Hu, M.: Mixture of sulfate and nitrate in coastal atmosphere aerosol :individual particle studies in Qingdao, China, Atmos. Environ., 374, 2669–2679, 2000.

Zhuang, H., Chan, C. K., Fang, M., and Wexler, A. S.: Formation of nitrate and non-sea-salt sulfate on coarse particles, Atmos. Environ., 33, 4223–4233, 1999.